Liver Damage Preferentially Results from CD8$^+$ T Cells Triggered by High Affinity Peptide Antigens

By Jennifer Q. Russell, Gregory J. Morrissette, Mark Weidner, Chirag Vyas, Deborah Aleman-Hoey, and Ralph C. Budd

From the Immunobiology Program, Department of Medicine, The University of Vermont College of Medicine, Burlington, Vermont 05405

Summary

Little is understood of the anatomical fate of activated T lymphocytes and the consequences they have on the tissues into which they migrate. Previous work has suggested that damaged lymphocytes migrate to the liver. This study compares class I versus class II major histocompatibility complex (MHC)–restricted ovalbumin-specific T cell antigen receptor (TCR) transgenic mice to demonstrate that after in vivo activation with antigen the emergence of CD4$^-$CD8$^-$B220$^+$ T cells occurs more frequently from a CD8$^+$ precursor than from CD4$^+$ T cells. Furthermore, this change in phenotype is conferred only by the high affinity native peptide antigen and not by lower affinity peptide variants. After activation of CD8$^+$ cells with only the high affinity peptide, there is also a dramatically increased number of liver lymphocytes with accompanying extensive hepatocyte damage and elevation of serum aspartate transaminase. This was not observed in mice bearing a class II MHC–restricted TCR. The findings show that CD4$^-$CD8$^-$B220$^+$ T cells preferentially derive from a CD8$^+$ precursor after a high intensity TCR signal. After activation, T cells can migrate to the liver and induce hepatocyte damage, and thereby serve as a model of autoimmune hepatitis.

Key words: liver lymphocytes • autoimmune hepatitis • T cell development • apoptosis • T cell antigen receptor transgenic mice

The activation of lymphocytes is accompanied by numerous changes in surface phenotype. Many of these changes, such as increased surface LFA-1 and the hyaluronate receptor/memory marker CD44, as well as decreased L-selectin (1), are critical to lymphocyte homing. Lymphocyte activation also results in clonal expansion, often followed by cell death through Fas-dependent apoptosis (2, 3). In some instances of T lymphocyte apoptosis, there may be an accompanying change in surface phenotype with downmodulation of CD4 or CD8 and upregulation of the B cell isoform of CD45 known as B220 (4, 5).

Collectively, the dynamic alterations in the trafficking of lymphocytes allow binding to vascular endothelium and the subsequent egress to extravascular tissues. The fate of lymphocytes once they have extravasated into tissues is less well understood, as are the consequences to the tissues that are infiltrated. The liver is a good model system in which to examine these events, as it contains a significant population of T cells expressing a previously activated phenotype, including expression of CD44, and in some instances a significant proportion of cells manifesting the phenotype CD4$^-$CD8$^-$B220$^+$ TCR-$\alpha/\beta^{intermediate}$ (4, 6). The origin of the latter population is unresolved. Some studies have argued that this subset represents a proliferating T cell population whose lineage is unique to the liver (7), whereas other investigations suggest that cells of the same phenotype might migrate to the liver after activation elsewhere, and undergo apoptosis within the liver (4). The lack of any significant expression of recombination-activating gene RAG-1 or RAG-2, proteins essential for rearrangement of the TCR α and β chains, by murine liver lymphocytes also argues against the adult liver being a site of T lymphocyte development (8). A third, although not mutually exclusive, view has shown that a subset of CD4$^-$CD8$^-$ and CD4$^+$ T cells that express the natural killer marker NK1.1 use a highly limited TCR repertoire (Vα14, Vβ8.2, Vβ7, or Vβ2) and are restricted in their response to the class I–like molecule CD1 (9).

We have previously proposed a model whereby CD4$^-$CD8$^-$B220$^+$TCR-α/β^+ cells result from a high intensity TCR signal that leads in most instances to apoptosis (10). A large proportion of the precursors of this subset are probably previously expressed CD8, as reflected by demethylation of the CD8α gene in CD4$^-$CD8$^-$TCR-α/β^+ cells in the thymus (11) and periphery (12). The further observation that mice lacking class I MHC expression are nearly devoid of CD4$^-$CD8$^-$TCR-α/β^+ cells (13–15) suggests that these unusual cells require an active signal conferred by class I MHC. In this study this model has been tested in two different TCR

 J. Exp. Med. © The Rockefeller University Press • 0022-1007/98/09/1147/11 $2.00
Volume 188, Number 6, September 21, 1998 1147–1157
http://www.jem.org

transgenic mice that recognize chicken OVA restricted to either class I MHC (OT-1 mice) or class II MHC (DO.11.10 mice). Our findings demonstrate that after equivalent doses of the appropriate OVA peptide, only the $CD8^+$ T cells from OT-1 mice showed increased expression of surface B220, with a portion becoming $CD4^-CD8^-$. The activated $CD8^+$ OT-1 T cells also migrated to the liver in considerably higher numbers and produced more hepatocyte damage than did activated $CD4^+$ cells in DO.11.10 mice. These findings were not observed in OT-1 mice that received lower affinity variants of the native OVA peptide. This suggests a model of autoimmune hepatitis in which stimulation of the T lymphocytes can occur at distant lymphoid sites, with subsequent migration to the liver where they provoke hepatocyte injury.

Materials and Methods

Mice. Normal strains of C57BL/6 and BALB/c mice and transgenic DO.11.10 or OT-1 mice were bred at the animal facilities of The University of Vermont College of Medicine. Original breeding pairs of normal mice were obtained from The Jackson Laboratory (Bar Harbor, ME). DO.11.10 TCR transgenic mice recognize chicken OVA peptide 323–339 in the context of class II MHC, $I\text{-}A^d$, and were the gift of Dr. Dennis Loh (Washington University, St. Louis, MO; reference 16). DO.11.10 mice were maintained by breeding transgenic male mice to normal BALB/c females. Offspring bearing the TCR transgene were identified by expression of the clonotype TCR identified by mAb KJ1-26. OT-1 mice bear a transgenic TCR that recognizes chicken OVA peptide 257–264 restricted to class I MHC, K^b, and were provided by Drs. Francis Carbone (Monash University Medical School, Victoria, Australia) and Michael Bevan (University of Washington, Seattle, WA; reference 17). OT-1 mice were maintained by breeding TCR transgenic male mice to normal C57BL/6 females. Offspring were screened for the clonotype TCR using anti-Vα2 mAb.

Antibodies, Cell Preparations, and Flow Cytometry. Monoclonal anti–murine CD8α conjugated to Red613 and PE-conjugated B220 were purchased from Caltag Labs. (Burlingame, CA). Monoclonal anti–murine CD4 conjugated to Red613 was purchased from GIBCO BRL (Gaithersburg, MD). Monoclonal anti–murine Vα2 conjugated to FITC or PE was purchased from PharMingen (San Diego, CA). The hybridoma KJ1-26, which reacts to the clonotype TCR of DO.11.10 mice, was the gift of Dr. Philippa Marrack (National Jewish Center for Immunology and Respiratory Diseases, Denver, CO). KJ1-26 was purified from mouse ascites on HiTRAP Protein G columns (Amersham Pharmacia Biotech, Inc., Piscataway, NJ), and then conjugated to fluorescein (Sigma Chemical Co., St. Louis., MO) using established methods (18). Fluorescein-conjugated antibody was purified from reaction components by chromatography on PD-10 columns (Amersham Pharmacia Biotech., Inc.).

Single cell suspensions were made by homogenizing tissues in RPMI 1640 medium (GIBCO BRL) supplemented with 5% (vol/vol) bovine calf serum (BCS)[1] (Hyclone Laboratories, Logan, UT). Cells excluding trypan blue were counted. For flow cytometry, 10^6 cells were incubated in 0.1 ml PBS containing 0.5% BSA Fraction V, 0.001% (wt/vol) sodium azide (Sigma Chemical Co.), and the antibodies listed above (3 μg/ml) at 4°C for 30 min (PBS azide). After washing with PBS-azide, cells were fixed in 1% (vol/vol) methanol-free formaldehyde (Ted Pella Inc., Reading, CA) in PBS-azide. Samples were stored at 4°C until they were analyzed with a Coulter Elite flow cytometer calibrated using DNA check beads (Coulter, Inc., Hialeah, FL). Apoptosis was quantified using staining with FITC-conjugated Annexin V (Nexins Research B.V., Hoeven, The Netherlands), which binds to phosphatidylserine residues that are found on the inner leaflet of cytoplasmic membranes of living cells but translocate to the outer leaflet upon initiation of apoptosis (19). Data were gated using Elite software by forward and side light scatter. Negative controls were set by using isotype-matched Ig directly conjugated to fluorochromes (Caltag Labs.).

OVA Peptides and Treatment of TCR Transgenic Mice. Peptides to chicken OVA 323–339 (ISQAVHAAHAEINEAGR) (OVA_{II}), 257-264 (SIINFEKL) (OVA_I), or OVA_I variants E1(EIINFEKL) and R4 (SIIRFEKL) were produced at Macromolecular Resources (Colorado State University, Fort Collins, CO). OVA_I/K^b binds to the OT-1 TCR with high affinity (K_d = 6.5 μM), whereas E1 and R4 bind with lesser affinities of 22.6 and 57.1 μM, respectively (20). $OVA_{II}/I\text{-}A^d$ binds to the DO.11.10 TCR with a K_d of 31 μM (21). Mice received one, two, or three daily intraperitoneal injections of 250 μl of 100-μM peptide solutions in PBS or PBS alone. Tissues were harvested 1, 2, 3, 5, or 7 d after the last injection of peptide.

Isolation of Liver Lymphocytes. After death, the peritoneal cavity was opened and the portal vein was identified. This was cannulated with a 27-gauge needle and perfused with 5 ml PBS until all the lobes of the liver blanched. With the needle remaining in the portal vein, the inferior vena cava was cut above the liver. The liver was then excised with forceps and the gall bladder was identified and removed. The liver was washed once in RPMI/5% BCS and then cut into small pieces and homogenized in a tissue grinder. Cells were then spun once at 1,200 rpm for 10 min. Supernatant was removed and the cells were resuspended in 10 ml of digestion mix consisting of serum-free RPMI containing 0.05% collagenase IV and 0.002% DNAse I (both from Sigma Chemical Co.), and then they were incubated at 37°C for 40 min, mixing the tube frequently. 30 ml of serum-free RPMI was then added and spun at 300 rpm for 3 min. This sedimented the majority of hepatocytes but left lymphocytes in the supernatant. The supernatant was transferred to another 50-ml tube and spun at 1,200 rpm for 10 min. The supernatant was aspirated and the cells were then resuspended in a total volume of 1.6 ml serum-free RPMI and transferred to a 15-ml tube. 2.4 ml of 40% (wt/vol) metrizamide (Sigma Chemical Co.) in PBS was added to the cells and mixed well. This solution was underlaid with 1 ml serum-free RPMI and spun at 2,500 rpm for 20 min. Liver lymphocytes were identified at the interface, carefully aspirated with a pasteur pipette, and transferred to another 15-ml tube, then washed with RPMI/5% BCS and spun at 1,600 rpm for 10 min. Cells were then resuspended in RPMI/5% BCS for analysis or placed in culture in complete medium (RPMI 1640, 5% FCS, 25 mM Hepes, 292.3 μg/ml glutamine, 2,500 μg/ml glucose, 10 μg/ml folate, 110.4 μg/ml pyruvate, 5×10^{-5} M 2-ME, 100 U/ml penicillin, and 100 U/ml streptomycin).

Results

Trafficking of $CD8^+$ T Cells to the Liver Is Induced only by High Affinity Peptide Antigen. To assess the relative dynam-

[1]*Abbreviations used in this paper:* AST, aspartate transaminase; BCS, bovine calf serum; OVA_I, OVA peptide SIINFEKL restricted to $H\text{-}2K^b$; OVA_{II}, OVA peptide ISQAVHAAHAEINEAGR restricted to $I\text{-}A^d$.

ics and consequences of $CD8^+$ versus $CD4^+$ T cell migration to the liver after antigen stimulation, two TCR transgenic mouse models were used, both of which recognize chicken OVA. T cells from OT-1 mice recognize OVA peptide 257–264 (OVA_I) restricted to class I MHC, K^b (17), whereas those from DO.11.10 mice recognize OVA peptide 323–339 (OVA_{II}) in the context of class II MHC, I-A^d (16).

A concentration range of OVA peptide was initially examined to determine what dose in vivo would produce a moderate increase of lymphocyte number in peripheral lymphoid tissues. In the case of OT-1 mice, 250 μl of 10-μM OVA_I produced only a slight increase in lymphoid number (data not shown), whereas 100-μM OVA_I produced a more substantial and reproducible increase and was consequently used in subsequent studies. A single administration of 250 μl of 100-μM OVA_I produced an abrupt decrease in thymocyte numbers by day 2, concomitant with a moderate twofold increase in lymph node cell numbers and little change in the number of splenocytes (Table 1, *Exp. no. 1*). During this period, the number of liver lymphocytes rose from a mean of 0.8 to 5.6 $\times$ 10^6. Less pronounced effects were observed with the lower affinity OVA peptide variants E1 and R4. The affinities of the OT-1 TCR for the E1/K^b complex (K_d = 22.6 μM) and R4–K^b complex (K_d = 57.1 μM) are reduced 3.5- and 8.8-fold, respectively, compared with native OVA_I (K_d = 6.5 μM) (20). Although a single dose of E1 and R4 produced a slight decrease in thymocyte numbers on day 2, there was otherwise only a modest increase in the size of peripheral lymphoid cell numbers by day 2, but no increase in the number of liver lymphocytes (Table 1, *Exp. no. 1*). This was also true even when E1 and R4 were administered three times at 24-h intervals (Table 1, *Exp. no. 3*).

Two doses of OVA_I resulted in a pronounced decrease of thymus size by day 2 and an increase in the number of lymph node cells and splenocytes, which peaked on day 3 (Table 1, *Exp. no. 2*). At the same time, there was a particular increase in the number of liver lymphocytes, which peaked on day 2. When administered at three 24-h intervals, OVA_I produced a profound increase (to 27 $\times$ 10^6) in the number of liver lymphocytes (Table 1, *Exp. no. 3*), but this dose also resulted in severe hepatic damage (see below). Thus, two 250-μl ad-

Table 1. *Kinetics of Lymphocyte Cell Numbers after Administration of OVA_I Peptide Variants to Class I–restricted (OT-1) OVA-specific TCR Transgenic Mice*

Exp. no.	Antigen	No. of doses	Day after antigen	Cell number $\times$ 10^6 ($\pm$ SD)			
				Thymus	Lymph node	Spleen	Liver
1	PBS	1	2	24.0 (9.1)	3.9 (1.3)	16.6 (6.5)	0.8 (0.14)
	OVA_I	1	1	9.6 (3.4)	7.2 (3.9)	23.4 (10.4)	1.9 (0.6)
	OVA_I	1	2	4.1 (2.7)	8.0 (7.9)	21.7 (23.6)	5.6 (0.14)
	E1	1	1	32.3 (2.2)	4.7 (0.99)	25.2 (10.2)	0.73 (0.59)
	E1	1	2	11.3 (6.8)	5.5 (4.1)	31.9 (13.1)	1.2 (0.25)
	R4	1	1	12.3 (1.02)	3.9 (5.9)	47.6 (14.2)	0.7
	R4	1	2	17.6	5.4	34.4	0.6
2	PBS	2	3	21.3 (4.4)	3.7 (1.9)	57.7 (4.9)	1.4 (0.1)
	OVA_I	2	2	1.8 (0.1)	7 .7 (1.7)	67.3 (22.2)	11.2 (1.8)
	OVA_I	2	3	4.5 (4.3)	11.0 (7.7)	80.2 (54.6)	6.3 (1.7)
	OVA_I	2	5 (1 died)	1.3 (1.5)	1.6 (0.8)	68.8 (92.3)	2.0 (0.1)
3	PBS	3	2	27.7 (2.7)	4.2 (0.84)	45.6 (0.57)	3.1 (0.99)
	OVA_I	3	2	2.0 (0.89)	4.6 (0.77)	37 (8.3)	26.4 (5.5)
	OVA_I	3	3	0.75 (0.35)	6.5 (0.71)	14.9 (13.6)	27.8 (15.2)
	OVA_I	3	5 (2 died)	3.2	1.2	13.6	9.5
	OVA_I	3	7	0.2 (0.5)	0.08 (0.04)	5.2 (3.4)	0.8 (1.2)
	E1	3	5	18	2.8	32.8	1.5
	R4	3	5	19.8	4.4	44.4	3.4

Female OT-1 mice (aged 10 wk in exp. no. 1, 18 wk in exp. no. 2, and 15 wk in exp. no. 3) received either 250 μl of PBS or 250 μl intraperitoneally of a 100-μM solution in PBS of the indicated peptide once daily for a total of one, two, or three doses. Peptides included either high affinity native OVA_I 257-264 (SIINFEKL, K_d = 6.5 μM), or single amino acid variants of lower affinity, E1 (EIINFEKL, K_d = 22.6 μM) or R4 (SIIRFEKL, K_d = 57.1 μM). Mice were examined on the indicated days after the last injection. Three mice were used for each condition, with the exception of exp. no. 3 where single mice received E1 or R4. Lymph node cell numbers reflect total yields from four nodes.

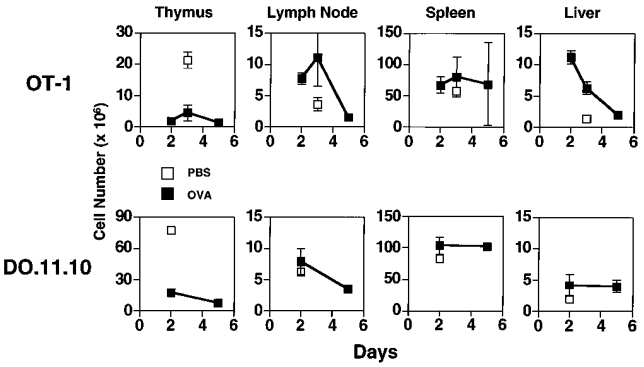

Figure 1. OVA antigen induces greater increase of liver lymphocytes in OT-1 than in DO.11.10 mice. OT-1 or DO.11.10 mice from experiment no. 2 received two doses of PBS or, respectively, OVA_I and OVA_{II} at 24-h intervals. Total lymphocyte numbers were determined for each organ on the day indicated after the last injection.

ministrations of 100-μM OVA_I were optimal for producing moderate expansion of peripheral lymphoid cell numbers and an increase in liver infiltration by lymphocytes.

Compared with the effects of OVA_I in OT-1 mice, the same doses of OVA_{II} administered to DO.11.10 mice yielded a similar loss of thymocytes and initial expansion of peripheral lymphoid tissues, but there was a somewhat less profound loss of lymphocytes at later time points (Tables 1 and 2 and Fig. 1). The DO.11.10 TCR binds OVA_{II}/I-A^d with an affinity of 31 μM (21). After OVA administration in both OT-1 and DO.11.10 mice, there was an initial expansion of lymph node cell number on days 2 and 3. After this, the rate and extent of decline in cell numbers was more pronounced in OT-1 mice. Thus, by day 5, lymph node and splenocyte cell numbers in OT-1 mice receiving OVA_I were the same as or considerably below those of control OT-1 mice, whereas peripheral lymphocyte cell numbers in DO.11.10 mice were often still above those of control mice. Similar differences were observed with three doses of the respective native OVA peptides (Tables 1 and 2).

Paralleling the temporal differences in lymphocyte loss between OT-1 and DO.11.10 mice after administration of their respective OVA peptides, both the kinetics and magnitude of lymphocyte accumulation in the liver were greater in the OT-1 mice. As mentioned above and shown in Table 1, after two doses of OVA_I, OT-1 liver lymphocyte numbers increased from a control of 1.4×10^6 to 11.2×10^6 on day 2, and after three doses of OVA_I this increased further to 27×10^6 on days 2 and 3. Thereafter, the degree of lymphocyte infiltration rapidly declined. In contrast, equivalent doses of OVA_{II} in DO.11.10 mice produced only modest increases in liver lymphocytes on day 2 and these continued to increase throughout days 5–7, although they never reached the magnitude seen in OT-1 mice (Table 2). The greater liver lymphocyte infiltrate in OT-1 mice was paralleled by an increased mortality in this group. At two doses, one out of nine OVA_I-treated OT-1 mice died on day 5, whereas at three doses, two out of nine mice died, also on day 5. No DO.11.10 mice died from OVA_{II} administration at any of the doses studied.

Cell Size Changes and Induction of $CD4^-CD8^-B220^+$ Phenotype in OT-1 T Lymphocytes after OVA_I Administration. In addition to the changes in the number of lymphocytes after administration of OVA_I, there were also sub-

Table 2. *Kinetics of Lymphocyte Cell Numbers after Administration of OVA_{II} Peptide to Class II–restricted (DO.11.10) OVA-specific TCR Transgenic Mice*

Exp. no.	Antigen	No. of doses	Day after antigen	Cell number × 10^6 (± SD)			
				Thymus	Lymph node	Spleen	Liver
1	PBS	1	2	81.1	6.8	87.2	2.4
	OVA_{II}	1	1	28.3	24.8	72.1	2.6
	OVA_{II}	1	2	30.3	14.8	63.6	6.8
2	PBS	2	2	77.5 (4.9)	6.2 (0.85)	82.2 (7.1)	2.0 (0.64)
	OVA_{II}	3	2	17.8 (0.85)	7.9 (3.0)	104 (19.8)	4.2 (2.4)
	OVA_{II}	3	5	7.8 (2.5)	3.5 (0.14)	101 (7.8)	4.0 (1.4)
3	PBS	3	3	74.5	5.6	77.2	1.5
	OVA_{II}	3	3	21.6	35.6	76	4.8
	OVA_{II}	3	5	16.8	14.1	98.3	6.1
	OVA_{II}	3	7	30.4	10.4	52.2	6.4

18–20-wk-old DO.11.10 mice received either 250 μl of PBS or 250 μl intraperitoneally of a 100-μM solution in PBS of OVA_{II} 323–339 (ISQAVHAAHAEINEAGR) once daily for a total of one, two, or three doses. Mice were examined on the indicated days after the last injection. Lymph node cell numbers reflect the total from four nodes. Single mice were used for each condition in exp. no. 1 and no. 3, and two mice per condition for exp. no. 2.

stantial changes in their morphology and phenotype. We (10) and others (22) have considered that the $CD4^-CD8^-$ phenotype for T cells reflects those that have received a high intensity TCR signal and are prone toward apoptosis. A useful additional marker for dying T cells is B220, the high molecular weight B cell isoform of CD45 (4). Thus, expression of B220 and loss of CD4 and CD8 were used along with cell size and Annexin V staining of apoptosis to determine the phenotype and fate of lymphocytes after treatment of OT-1 and DO.11.10 mice with OVA.

The shifts in cell size and phenotype after administration of OVA peptides were also more dramatic in the OT-1 mice than in DO.11.10 mice. Although most of the TCR transgenic $V\alpha2^+$ cells in lymphoid tissues of control OT-1 mice were $CD8^+$, after OVA_I there was a large but transient increase in the proportion of peripheral $CD4^-CD8^-V\alpha2^+$ cells. A striking shift from $CD8^+$ to $CD4^-CD8^-$ could be seen as soon as 1 d after administration of only the high affinity OVA_I peptide. As shown in Fig. 2, the low and moderate affinity OVA_I variants, R4 and E1, respectively, produced little or no substantial change from PBS-injected control mice in the phenotypic composition of the lymph nodes, which were predominantly $CD8^+$ and manifested only 8–9% surface B220. However, within 24 h of a single dose of OVA_I there was a decrease in the proportion of $CD8^+$ cells, from 60% with PBS to 28% with OVA_I. Accompanying this was a reciprocal increase in the proportion of $CD4^-CD8^-$ cells, from 35% with PBS to 69% with OVA_I, 45% of which were $V\alpha2^+$ (Fig. 2). These phenotypic shifts were confirmed by absolute numbers. The number of $CD8^+V\alpha2^+$ cells decreased only after treatment with OVA_I. The number of $CD4^-CD8^-V\alpha2^+$ lymph node cells did not change with R4 and increased nearly twofold with E1, whereas with OVA_I this subset increased fourfold. These changes in phenotype and cell number were very consistent in three separate experiments. In addition to the induction of $CD4^-CD8^-V\alpha2^+$ cells with OVA_I, the residual $CD8^+$ cells after OVA_I treatment now expressed increased amounts of B220 (24%). B220 expression by the $CD4^-CD8^-V\alpha2^+$ subset was already significant before antigen exposure (62–78%) and did not increase any further after OVA_I administration (Fig. 2). This may reflect the fact that the $CD4^-CD8^-$ T cells in normal mice have also arisen by a high intensity TCR signal from endogenous or environmental antigens.

Various sized lymphoid populations appeared in rapid succession after two doses of OVA_I to OT-1 mice, as shown for lymph node cells in Fig. 3. On day 2 a blast population was observed that was enriched in the proportion of $CD4^-CD8^-V\alpha2^+$ cells compared with control OT-1 mice. This increase occurred at the expense of the $CD8^+$ subset, which on day 2 diminished from 63 to 43%, but at the same time manifested increased B220 expression (34%) compared with control mice (17%) (Fig. 3 *A*). Concomitantly, a subpopulation of small cells gradually increased during the 5 d after administration of OVA_I. As shown in Fig. 3 *B*, these small cells were considerably enriched in the proportion of $CD4^-CD8^-B220^+V\alpha2^+$ cells, even in PBS-treated control mice. Furthermore, the minor $CD8^+$ subset also expressed more B220 than was seen in the blast cells. These morphologic and phenotypic changes corresponded to an initial expansion in peripheral lymphoid cell numbers

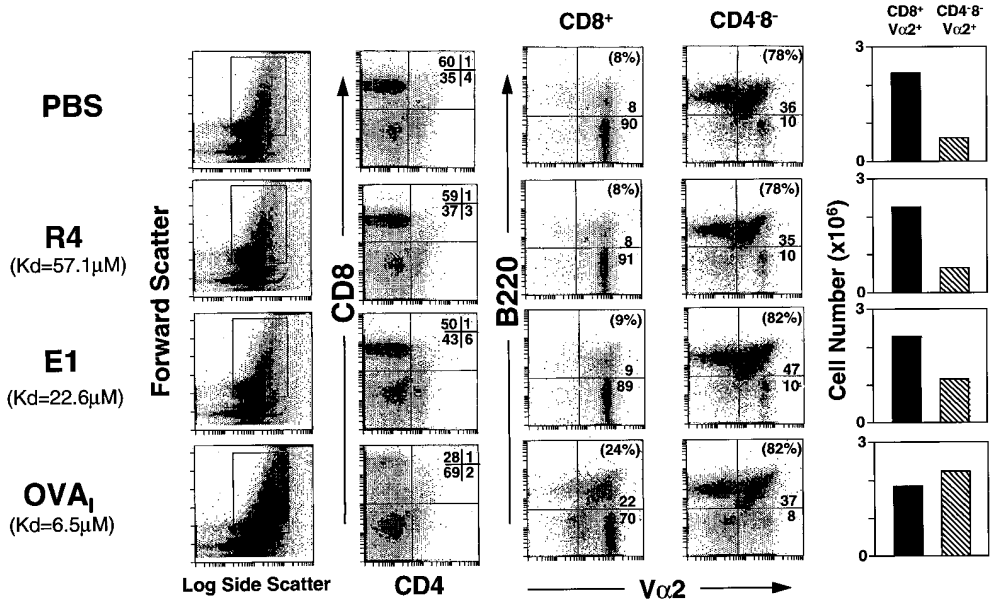

Figure 2. Induction of $CD4^-CD8^-V\alpha2^+$ and $CD8^+B220^+$ phenotype only by high affinity OVA_I peptide. OT-1 mice, three per group, received a single injection of the indicated peptide or PBS. OVA_I confers a high affinity (K_d = 6.5 μM) interaction with the OT-1 TCR when complexed with K^b. R4 and E1 are OVA_I variants that manifest affinities of 57.1 and 22.6 μM, respectively. On day 1 after injections, lymph node cells from each group were pooled and analyzed for expression of CD4, CD8, Vα2, and B220. Numbers in quadrants indicate the percentage of positive cells. The forward and side scatter histograms at the left show that the gates set for this analysis were uniform and did not include small dying cells. Numbers in parentheses represent the percentage of $V\alpha2^+$ cells that express B220. The right hand column displays absolute numbers of $CD8^+V\alpha2^+$ and $CD4^-CD8^-V\alpha2^+$ cells. The findings are representative of three experiments.

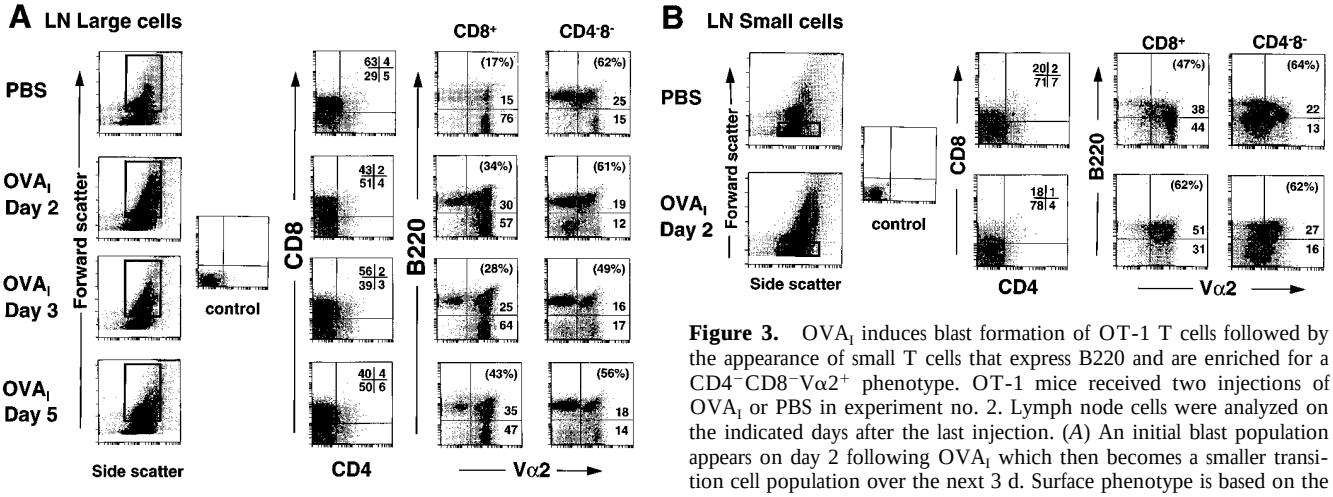

Figure 3. OVA$_I$ induces blast formation of OT-1 T cells followed by the appearance of small T cells that express B220 and are enriched for a CD4$^-$CD8$^-$Vα2$^+$ phenotype. OT-1 mice received two injections of OVA$_I$ or PBS in experiment no. 2. Lymph node cells were analyzed on the indicated days after the last injection. (*A*) An initial blast population appears on day 2 following OVA$_I$ which then becomes a smaller transition cell population over the next 3 d. Surface phenotype is based on the large and moderate sized cells as shown by the enclosed gate. (*B*) The small sized population of lymphocytes is enriched for CD4$^-$CD8$^-$Vα2$^+$B220$^+$ cells. OVA$_I$ administration also increased the proportion of CD8$^+$ cells expressing B220.

by day 2 followed by a rapid decline by day 5 in OT-1 mice that had received OVA$_I$ (Fig. 4 *A*). Throughout this period there was an increase in the expression of B220 by the CD8$^+$ subset in thymus, lymph node, and spleen (Fig. 4 *B*). In contrast to OT-1 mice, the appearance of CD4$^-$CD8$^-$ B220$^+$ T cells did not occur in DO.11.10 mice at the same dose of OVA$_{II}$ (Fig. 5). In fact, the absolute number of CD4$^-$CD8$^-$KJ1-26$^+$ cells often decreased with OVA$_{II}$, whereas the number of CD4$^+$ lymph node cells increased. Even at a 100-fold higher dose of OVA$_{II}$ there was still no significant induction of B220 expression by T cells, nor of CD4$^-$CD8$^-$ T cells (data not shown).

Liver Lymphocyte Phenotype. By contrast with other lymphoid tissues, after OVA$_I$ treatment of OT-1 mice the liver lymphocytes contained an initial dramatic increase in the proportion and absolute number of CD8$^+$Vα2$^+$ and CD4$^-$CD8$^-$Vα2$^+$ cells (Fig. 4 *A*). This caused the ratio of CD4$^-$CD8$^-$Vα2$^+$ to CD8$^+$Vα2$^+$ cells to decrease rather than increase as observed in the lymph nodes (compare Figs. 2 and 6). However, by day 5 the proportion of CD8$^+$ cells had decreased to nearly their initial levels, with a somewhat slower decline in the proportion of CD4$^-$CD8$^-$ Vα2$^+$ cells. In addition, after OVA$_I$ administration the liver lymphocytes did not manifest significant B220 expression in either the CD8$^+$ or CD4$^-$CD8$^-$ subsets over the 5-d course of the experiment. These findings suggested that migration of lymphocytes to the liver was a selective process in OT-1 mice, initially of activated CD8$^+$ cells; however, they may have changed their phenotype to CD4$^-$CD8$^-$ within the liver.

Annexin V staining confirmed that lymphocytes in the liver were undergoing increased apoptosis. Fig. 7 *A* displays Annexin V staining from experiment no. 3 and illustrates that the resident CD8$^+$ liver lymphocytes in OT-1 mice contained a higher proportion of Annexin V$^+$ cells (57.1%) than either lymph node (13.8%) or spleen (11.9%, data not shown). After OVA$_I$ administration, there was a significant increase on day 2 of Annexin V$^+$ CD8$^+$ cells in lymph node (42.8%) and spleen (34.4%, data not shown), which decreased only partially by day 5. In contrast, the liver lymphocytes maintained an already high proportion of Annexin V$^+$ CD8$^+$ cells (58.8%). By day 5, the Annexin V$^+$ subset of

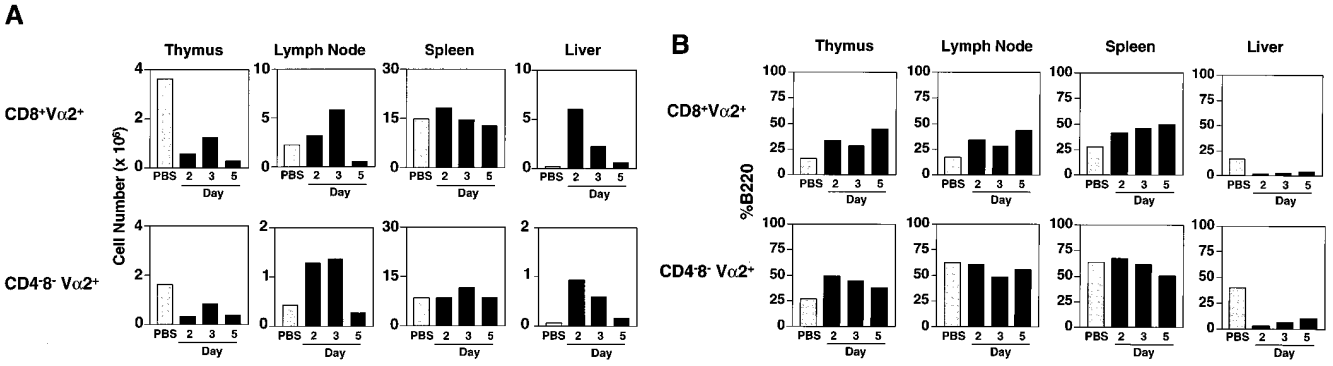

Figure 4. Cell counts and percentage of B220 expression by the CD8$^+$Vα2$^+$ and CD4$^-$CD8$^-$Vα2$^+$ subsets of T cells from OT-1 mice after two doses of OVA$_I$. Analysis is based on the same mice as used in experiment no. 2 in Fig. 1 and phenotypes were determined on the living cells based on flow cytometric size gates. Tissues were pooled from three OT-1 mice per group. (*A*) Actual lymphocyte counts of subsets in various organs. (*B*) Percentage of cells in the indicated subset that expressed B220.

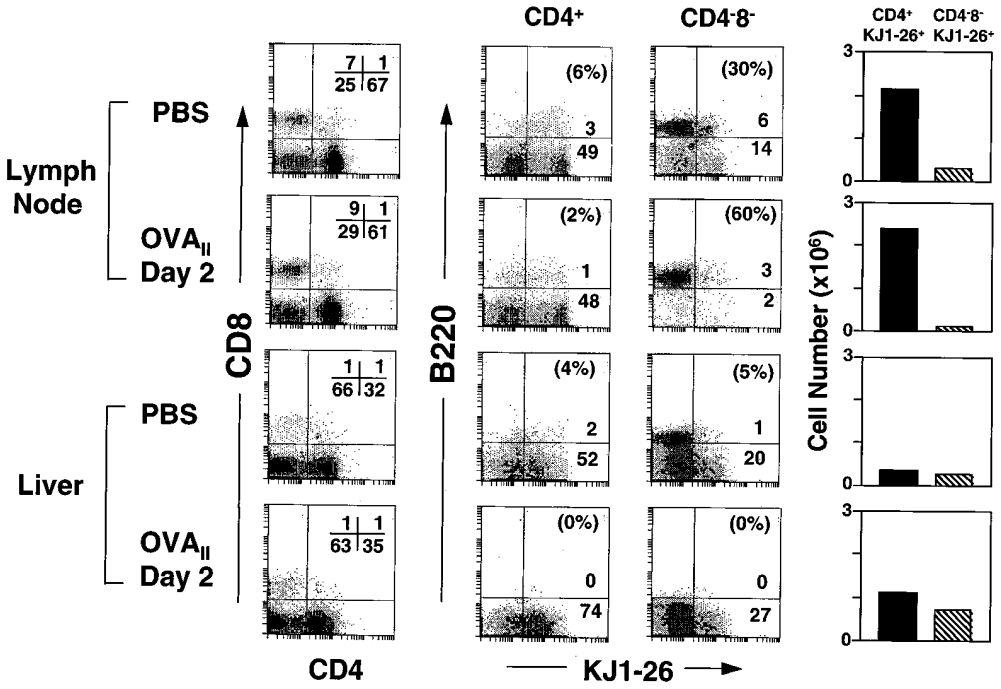

Figure 5. OVA_{II} does not induce B220 expression or $CD4^-CD8^-$ phenotype by responding $CD4^+$ cells from DO.11.10 mice. DO.11.10 mice received OVA_{II} injections and lymph node cells (*top*) or liver lymphocytes (*bottom*) were examined for expression of CD4, CD8, B220, and clonotype TCR using antibody KJ1-26. The right column indicates the absolute numbers of KJ1-26^+ cells that were $CD4^+$ or $CD4^-CD8^-$. Phenotypes were based on gates set for living cells as in Fig. 2.

$CD8^+$ liver lymphocytes had decreased to levels seen in the periphery, and were clearly less than was observed in liver lymphocytes from control mice. As before, DO.11.10 mice demonstrated less evidence of lymphocyte apoptosis after OVA_{II} (Fig. 7 *B*). Although DO.11.10 liver lymphocytes revealed more apoptosis than lymph node cells from the same mice, these levels did not approach those seen in OT-1 mice. The findings were similar in two other experiments.

Infiltrating $CD8^+$ Liver Lymphocytes Induce Hepatocyte Death. Similar to the more profound influx of liver lymphocytes in OT-1 mice versus DO.11.10 mice after OVA treatment, serum levels of the hepatocyte enzyme aspartate transaminase (AST) rose dramatically in OT-1 mice, but not at all in DO.11.10 mice. As shown in Table 3, AST elevation was maximal and statistically significant on day 2 in OT-1 mice ($P = 0.030$), which corresponded to the time of greatest numbers of liver lymphocytes.

Because serum AST elevation parallels hepatocyte injury, liver histology was examined before and after OVA administration to assess the degree of hepatocyte damage. Fig. 8 shows hematoxylin and eosin–stained liver sections from OT-1 mice (*left*) and DO.11.10 mice (*right*). Livers from nontransgenic C57BL/6 mice that received OVA_I peptide (Fig. 8 *A*) and from BALB/c mice that received OVA_{II} (Fig. 8 *F*) showed a normal morphology of hepatocytes with few lymphocytes in the liver sinusoids. Similarly, PBS administration to OT-1 mice (Fig. 8 *B*) and DO.11.10 mice (Fig. 8 *G*) had similar normal appearances. However, there was an intense infiltration of liver lymphocytes over the 5 d after OVA_I administration to OT-1 mice. On day 2 there was a prominent infiltrate that was confined to the periportal region (Fig. 8 *C*). By day 3 this had progressed to an intense pansinusoidal infiltration of lymphocytes accompanied by extensive hepatocyte damage (Fig. 8 *D*). Thus, the peak of observed hepatocyte damage histologically occurred 24 h after the peak serum AST elevations. By day 5 the lymphocyte infiltrate was largely resolved (Fig. 8 *E*). Accompanying this recovery was the appearance of massive levels of hepatocyte mitosis (Fig. 8, *E* and *J*). Although DO.11.10 mice also manifested periportal lymphocytic infiltrates on day 2 after OVA_{II} (Fig. 8 *H*), these quickly dissipated as liver lymphocytes became more loosely scattered throughout the liver on days 3–5 (Fig. 8 *I*). Throughout this process there was no evidence of hepatocyte injury in DO.11.10 mice.

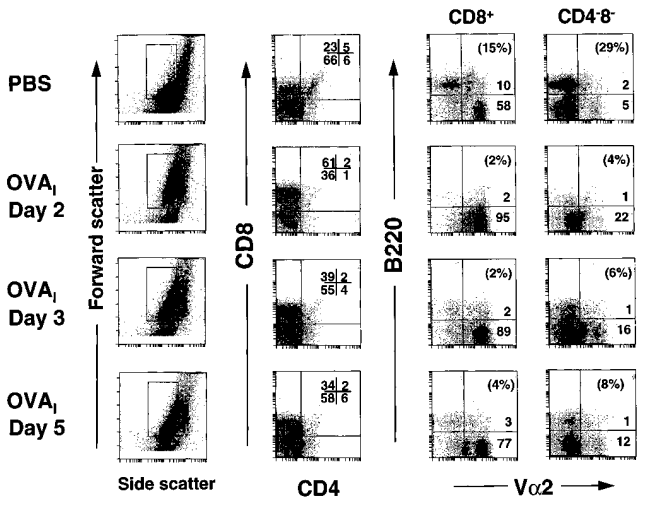

Figure 6. Some resident liver T lymphocytes in OT-1 mice express B220, but after OVA_I administration the initial influx is of $CD8^+$ cells that lack B220. OT-1 mice received two injections of OVA_I in experiment no. 2 and liver lymphocytes were isolated on the indicated days after the last injection. The forward and side scatter histograms at the left show that the gates set for this analysis were uniform and did not include small dying cells.

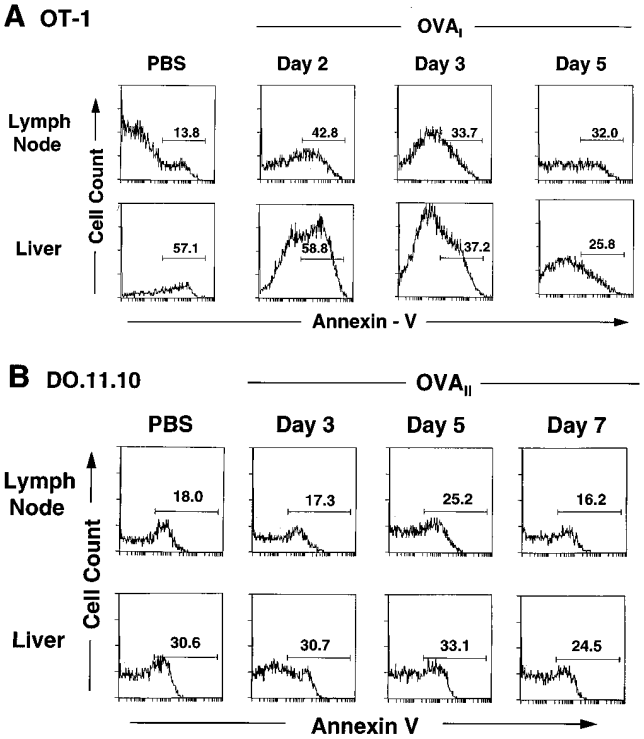

Figure 7. Liver lymphocytes and lymph node cells are undergoing increased apoptosis in OT-1 mice compared with DO.11.10 mice. Mice are from experiment no. 3 and received three doses of PBS, OVA_I (OT-1 mice), or OVA_{II} (DO.11.10 mice) at 24-h intervals. Lymphoid cells were isolated at the indicated time points and stained with Annexin V and either anti-CD8 (for OT-1 mice) or anti-CD4 (for DO.11.10 mice). Analysis is gated on $CD8^+$ cells from OT-1 mice (*A*) or on $CD4^+$ cells from DO.11.10 mice (*B*).

Discussion

Our findings support a model in which the liver is a destination for lymphocytes that have been activated by a high intensity TCR signal, many of which are destined to undergo apoptosis. Although lymphocytes may not be actively undergoing apoptosis as they enter the liver, given the generally higher levels of Annexin V staining of intrahepatic lymphocytes compared with peripheral lymphoid tissues, it is most likely that a considerable portion are targeted for apoptosis after entry. In this study, this process appeared to be more dynamic for $CD8^+$ than $CD4^+$ T cells. Furthermore, the entry of activated $CD8^+$ lymphocytes into intrahepatic sinusoids was responsible for extensive hepatocyte death.

Table 3. *Elevation of Serum AST after Activation of OT-1 $CD8^+$ Cells*

Mouse strain	Antigen	Days after antigen	Mean (± SD) serum AST
			U/liter
OT-1	PBS	2	172 (84.4)
	OVA_I	2	586 (153) [$P = 0.030$]
	OVA_I	3	197 (82.6)
	OVA_I	5	174 (5.7)
C57BL/6	OVA_I	2	119 (38.9)
DO.11.10	PBS	2	126 (55.2)
	OVA_{II}	2	115 (34.6)
	OVA_{II}	5	97.5 (14.8)

Three OT-1 mice and two DO.11.10 mice received, respectively, OVA_I and OVA_{II} administered as two 250 μl intraperitoneal doses of a 100-μM solution at 24-h intervals. As a control for nonspecific effects of the OVA_I peptide, two nontransgenic C57BL/6 mice received the same dose of OVA_I. Serum AST levels were determined at the indicated times after administration of antigen. The only group with significantly elevated AST levels compared to PBS control mice was day 2 OT-1 mice ($P = 0.030$, paired Student's *t* test).

The notion that "damaged" lymphocytes might not traffic normally to peripheral lymphoid tissues but might rather migrate to the liver has been appreciated for some time. Treatment of lymphocytes with trypsin (23) or glycosidases (24) before intravenous infusion prevented the cells from circulating normally. After neuraminidase treatment of lymphocytes to remove terminal sialic acid residues, the cells selectively migrated to the liver (25). Conceivably, recognition of such altered lymphocytes might occur via the asialoglycoprotein receptor expressed by hepatocytes (26). One of the early events in apoptosis is the expression of surface phosphatidylserine residues on the outer surface of the plasma membrane, which are normally confined to the inner leaflet (19). Receptors for phosphatidylserine are expressed by macrophages such as the Kupffer cells in the liver (27). This might further enhance the tendency of T cells that are targeted for apoptosis to migrate to the liver. It is conceivable that the abrupt increase in OT-1 liver lymphocytes following administration of OVA_I might represent clonal expansion of resident liver lymphocytes rather than migration to the liver. However, this is unlikely as the fold increase of liver lymphocytes vastly surpassed that of peripheral lymphocytes.

Figure 8. Infiltration of lymphocytes into the liver and resulting hepatocyte damage after OVA administration are both more pronounced in OT-1 mice than DO.11.10 mice. Livers were taken from mice of experiment no. 2 that had received two doses of OVA and were stained with hematoxylin and eosin. Original magnification is ×160 except for J, which is ×1,000. Administration of OVA_I to nontransgenic C57BL/6 mice (*A*) and OVA_{II} to nontransgenic BALB/c mice (*F*) yielded no influx of liver lymphocytes and no hepatocyte damage. Similarly, PBS administration to OT-1 mice (*B*) or DO.11.10 mice (*G*) also produced no infiltrates. Beginning on day 2 after administration of OVA_I to OT-1 mice or OVA_{II} to DO.11.10 mice, periportal lymphocytic infiltrates were observed in both mice but were more intense in OT-1 (*C*) than DO.11.10 mice (*H*). By day 3 a massive lymphocytic infiltrate is observed throughout the livers of only OT-1 mice with extensive hepatocyte damage (*D*). By day 5 the lymphocytic infiltrate in OT-1 livers is resolved (*E*) and in its wake is observed a dramatic burst of hepatocyte mitotic activity, shown magnified in *J*. By contrast, DO.11.10 mice never manifested extensive liver sinusoidal lymphocytes as infiltrates were completely gone by day 5 without any evidence of hepatocyte damage or mitotic rebound (*I*).

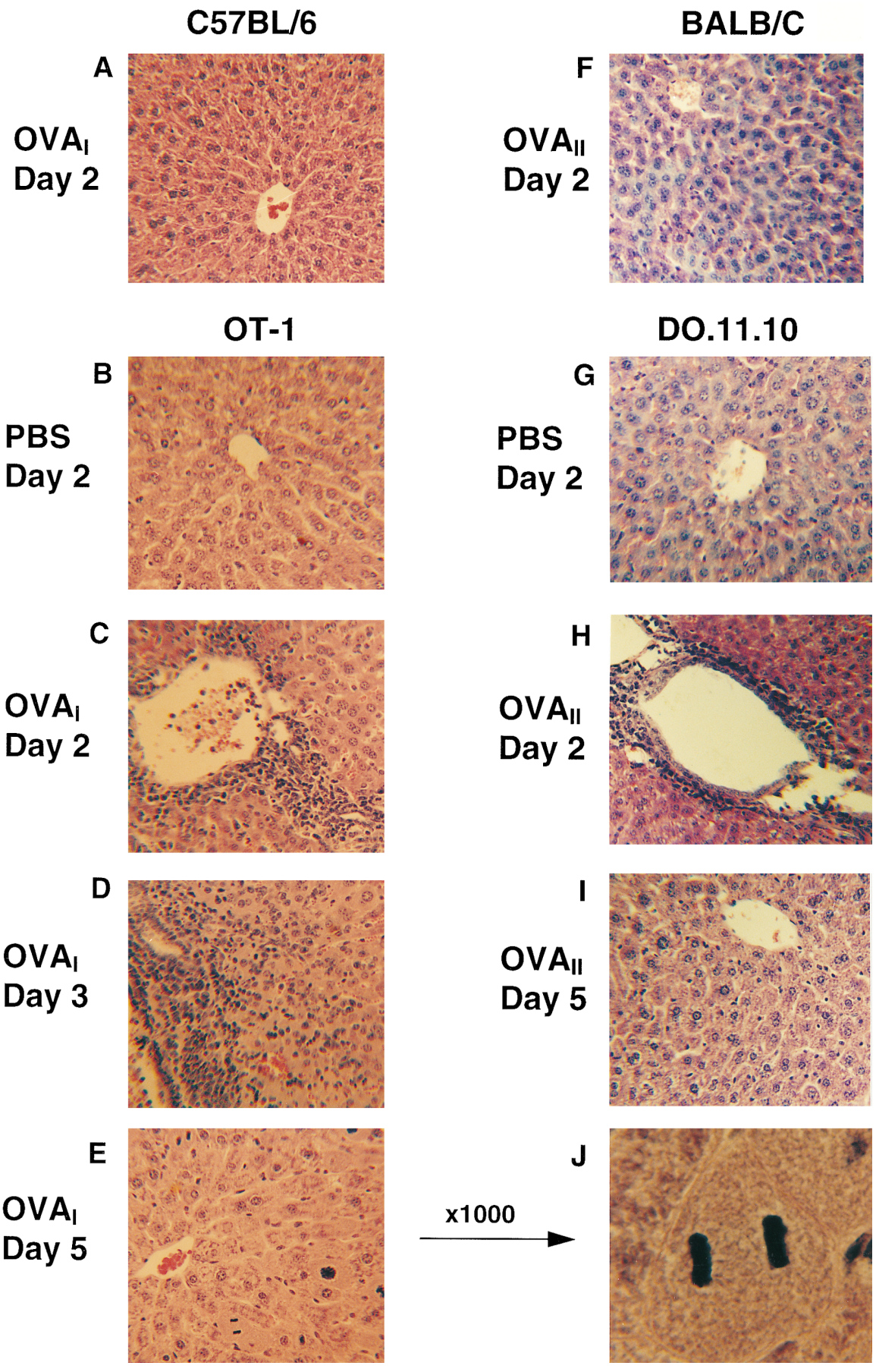
C57BL/6
BALB/C
A
OVA$_I$
Day 2
F
OVA$_{II}$
Day 2
OT-1
DO.11.10
B
PBS
Day 2
G
PBS
Day 2
C
OVA$_I$
Day 2
H
OVA$_{II}$
Day 2
D
OVA$_I$
Day 3
I
OVA$_{II}$
Day 5
E
OVA$_I$
Day 5
x1000
J

Furthermore, liver lymphocytes were not observed to be in the G2/S phase of the cell cycle by propidium iodide analysis (Russell, J.Q., unpublished observations). Thus, it is more likely that the activated lymphocytes migrated to the liver.

In this study, $CD8^+$ T cells from the class I MHC–restricted TCR transgenic OT-1 mouse manifested a considerably more dramatic influx into the liver with resulting hepatocyte damage after receiving OVA_I than did $CD4^+$ T cells from DO.11.10 mice after an equivalent dose of OVA_{II}. This was paralleled by a greater tendency for OT-1 $CD8^+$ T cells in lymph node and spleen to acquire B220 expression and to manifest a $CD4^-CD8^-$ phenotype than was demonstrated by DO.11.10 $CD4^+$ cells. These findings are in partial agreement with those of Huang et al. (4), which showed that after exposure to a class I MHC–restricted antigen, a portion of the responding peripheral $CD8^+$ T lymphocytes became $CD4^-CD8^-B220^+$. However, that study also observed that the T cells that migrated to the liver after antigen exposure were predominantly of the $CD4^-CD8^-B220^+$ phenotype. In contrast, we observed an influx of primarily $CD8^+$ cells with a smaller proportion of $CD4^-CD8^-$ T cells, although the absolute numbers of the latter population in the liver did increase considerably. The difference in these two systems may reflect that in OT-1 mice the large proportion of $CD4^-CD8^-B220^+$ T cells generated in the lymph nodes and spleen with OVA never reached the liver and died in situ or en route to the liver.

We (10) and others (22) have previously suggested that the $CD4^-CD8^-$ T cell phenotype reflects high intensity TCR signaling and a tendency to undergo apoptosis. This would be consistent with the findings that in OT-1 mice only the high affinity OVA_I peptide, and not the lower affinity E1 and R4 peptide variants, induced $CD4^-CD8^-$ $V\alpha2^+$ cells and concomitant liver damage. It is possible that the higher intensity signaling by OT-1 T cells was unique to this system and not applicable to $CD8^+$ versus $CD4^+$ T cells in general. In this regard, the OT-1 TCR has an affinity of 6.5 μM for OVA_I/K^b (20), whereas the affinity of the DO.11.10 TCR for $OVA_{II}/I\text{-}A^d$ is 31 μM (21). However, in other studies using class I– and class II–restricted TCR transgenic mice different from those used in this study, the findings also showed that the class I–restricted $CD8^+$ T cells manifested a much greater influx into the liver as well as a higher proportion of $CD4^-CD8^-B220^+$ T cells (Crispe, I.N., personal communication, and reference 4). Furthermore, as normal mice age the liver accumulates a greater proportion of $CD8^+$ and $CD4^-CD8^-$ T cells than of $CD4^+$ T cells (6). This may reflect merely an increased tendency of $CD8^+$ T cells to traffic to the liver after activation. Alternatively, the collective findings also agree with other studies of thymocyte development, suggesting that on average $CD8^+$ T cells may receive higher intensity signals than do $CD4^+$ cells (22).

It has been previously appreciated that infiltration of the liver by Con A–activated lymphocytes produces collateral liver damage (28). As such, that study and this may represent models of autoimmune hepatitis in which T lymphocytes become antigen activated in lymphoid organs and then migrate to the liver and cause hepatocyte apoptosis. Hepatocytes may be merely innocent bystanders in this system, having little if anything to do with actual antigen presentation. Hepatocytes express high levels of Fas and are highly susceptible to apoptosis induced by in vivo administration of anti-Fas antibody (29). However, in the Con A–induced liver injury model, it appears that perforin plays a more prominent role than Fas-mediated cell death (30). Studies are in progress to examine this issue in OT-1/*lpr* mice. This mechanism of lymphocyte-mediated tissue injury might also apply to other target organs and manifest itself as idiopathic autoimmune damage. In this system, antigen presentation by the target organ may not be necessary for either the trafficking of lymphocytes to the organ or the subsequent tissue injury induced by infiltrating lymphocytes. We (Russell, J.Q., unpublished observations) and others (31) have observed that antigen-activated T cells also traffic to the lung and kidneys and we are examining the degree of tissue injury that results at these sites. This model might also serve to explain the liver dysfunction that is often observed after situations where the immune system has been strongly activated, such as by a superantigen in Kawasaki disease (32, 33).

Beyond the parallels with autoimmune hepatitis, our findings may also have implications for normal liver homeostasis. The resident liver lymphocytes that are observed before intentional antigen challenge may have also migrated to the liver after activation by endogenous or environmental antigens. This constant low level influx of activated lymphocytes may result in a continual minimal degree of hepatocyte apoptosis. In this regard, it is interesting to note that liver enlargement due to actual increase in hepatocyte mass has been observed in Fas-deficient mice (34).

We wish to thank Allison Stout for technical assistance and Colette Charland for assistance with flow cytometry.

This work was supported by grant AI-36333 from the National Institutes of Health.

Address correspondence to Ralph C. Budd, The University of Vermont College of Medicine, Given Medical Bldg., Burlington, VT 05405-0068. Phone: 802-656-2286; Fax: 802-656-3854; E-mail: rbudd@zoo.uvm.edu

Received for publication 16 April 1998 and in revised form 17 June 1998.

References

1. Warnock, R.A., S. Askari, E.C. Butcher, and U.H. von Andrian. 1998. Molecular mechanisms of lymphocyte homing to peripheral lymph nodes. *J. Exp. Med.* 187:205–216.
2. Singer, G.G., and A.K. Abbas. 1994. The fas antigen is involved in peripheral but not thymic deletion of T lymphocytes in T cell receptor transgenic mice. *Immunity*. 1:365–371.
3. Ju, S.T., D.J. Panka, H. Cui, R. Ettinger, M. El-Khatib, D.H. Sherr, B.Z. Stanger, and A. Marshak-Rothstein. 1995. Fas(CD95)/FasL interactions required for programmed cell death after T-cell activation. *Nature*. 373:345–347.
4. Huang, L., G. Soldeville, M. Leeker, R. Flavell, and N. Crispe. 1994. The liver eliminates T cells undergoing antigen-triggered apoptosis in vivo. *Immunity*. 1:741–749.
5. Renno, T., M. Hahne, J. Tschopp, and H.R. MacDonald. 1995. Peripheral T cells undergoing superantigen-induced apoptosis in vivo express B220 and upregulate Fas and Fas ligand. *J. Exp. Med.* 183:431–437.
6. Ohteki, T., R. Okuyama, S. Seki, T. Abo, K. Sugiura, A. Kusumi, T. Ohmori, H. Watanabe, and K. Kumagai. 1992. Age-dependent increase of extrathymic T cells in the liver and their appearance in the periphery of older mice. *J. Immunol.* 149:1562–1570.
7. Ohteki, T., S. Seki, T. Abo, and K. Kumagai. 1990. Liver is a possible site for the proliferation of abnormal $CD3^+4^-8^-$ double-negative lymphocytes in autoimmune MRL-*lpr/lpr* mice. *J. Exp. Med.* 172:7–12.
8. Crispe, I.N., and L. Huang. 1994. Neonatal, moribund and undead T cells: the role of the liver in T cell deletion. *Semin. Immunol.* 6:39–41.
9. Bendelac, A., O. Lantz, M.E. Quimby, J.W. Yewdell, J.R. Bennink, and R.R. Brutkiewicz. 1995. CD1 recognition by mouse $NK1^+$ T lymphocytes. *Science*. 268:863–865.
10. Budd, R.C., and P.F. Mixter. 1995. The origin of $CD4^-CD8^-$ TCR-$\alpha\beta^+$ thymocytes: a model based on T cell receptor avidity. *Immunol. Today*. 16:428–431.
11. Takahama, Y., A. Kosugi, and A. Singer. 1991. Phenotype, ontogeny, and repertoire of $CD4^-CD8^-$ T cell receptor $\alpha\beta^+$ thymocytes. *J. Immunol.* 146:1134–1143.
12. Tutt-Landolfi, M.M., N. Van Houten, J.Q. Russell, R. Scollay, J. Parnes, and R.C. Budd. 1993. $CD2^-CD4^-CD8^-$ lymph node T lymphocytes in MRL *lpr/lpr* mice are derived from a $CD2^+CD4^+CD8^+$ thymic precursor. *J. Immunol.* 151: 1086–1096.
13. Bix, M., M. Coles, and D.H. Raulet. 1993. Positive selection of $V\beta8^+$ $CD4^-8^-$ thymocytes by class I molecules expressed by hematopoietic cells. *J. Exp. Med.* 178:901–904.
14. Mixter, P.F., J.Q. Russell, F.H. Durie, and R.C. Budd. 1995. Decreased $CD4^-CD8^-$ TCR-$\alpha\beta^+$ cells in *lpr/lpr* mice lacking β2-microglobulin. *J. Immunol.* 154:2063–2074.
15. Ohteki, T., and H.R. MacDonald. 1994. Major histocompatibility complex class I related molecules control the development of $CD4^+CD8^-$ and $CD4^-CD8^-$ subsets of natural killer 1.1^+ T cell receptor α/β^+ cells in the liver of mice. *J. Exp. Med.* 180:699–704.
16. Murphy, K.M., A.B. Heimberger, and D.Y. Loh. 1990. Induction by antigen of intrathymic apoptosis of $CD4^+CD8^+$ TCR^{lo} thymocytes in vivo. *Science*. 250:1720–1723.
17. Hogquist, K.A., S.C. Jameson, W.R. Heath, J.L. Howard, M.J. Bevan, and F.R. Carbone. 1994. T cell receptor antagonist peptides induce positive selection. *Cell*. 76:17–27.
18. Goding, J.W. 1983. Monoclonal Antibodies: Principles and Practice. Academic Press, New York, NY. 232–233.
19. Vermes, I., C. Haanen, H. Steffens-Nakken, and C. Reutelingsperger. 1995. A novel assay for apoptosis: flow cytometric detection of phosphatidylserine expression on early apoptotic cells using fluorescein labeled Annexin-V. *J. Immunol. Methods*. 184:39–51.
20. Munir Alam, S., P.J. Travers, J.L. Wung, W. Nasholds, S. Redpath, S.C. Jameson, and N.R.J. Gascoigne. 1996. T-cell receptor affinity and thymocyte positive selection. *Nature*. 381:616–620.
21. Seibel, J.L., N. Wilson, H. Kozono, P. Marrack, and J.W. Kappler. 1997. Influence of the NH_2-terminal amino acid of the T cell receptor α chain on major histocompatibility complex (MHC) class II + peptide recognition. *J. Exp. Med.* 185: 1919–1927.
22. Liu, C.-P., J.W. Kappler, and P. Marrack. 1996. Thymocytes can become mature T cells without passing through the $CD4^+$ $CD8^+$, double positive stage. *J. Exp. Med.* 184:1619–1630.
23. Woodruff, J., and B.M. Gesner. 1968. Lymphocytes: circulation altered by trypsin. *Science*. 161:176–178.
24. Gesner, B.M., and V. Ginsburg. 1964. Effect of glycosidases on the fate of transfused lymphocytes. *Proc. Natl. Acad. Sci. USA*. 52:750–756.
25. Woodruff, J.J., and B.M. Gesner. 1969. The effect of neuraminidase on the fate of transfused lymphocytes. *J. Exp. Med.* 129:551–567.
26. Bennatt, D.J., Y.Y. Ling, and D.D. McAbee. 1997. Isolated rat hepatocytes bind lactoferrins by the RHL-1 subunit of the asialoglycoprotein receptor in a galactose-independent manner. *Biochemistry*. 36:8367–8376.
27. Martin, S.J., C.P.M. Reutelingsperger, A.J. McGahon, J.A. Rader, R.C.A.A. van Schie, D.M. LaFace, and D.R. Green. 1995. Early redistribution of plasma membrane phosphatidylserine is a general feature of apoptosis regardless of the initiating stimulus: inhibition by overexpression of Bcl-2 and Abl. *J. Exp. Med.* 182:1545–1556.
28. Tiegs, G., J. Hentschel, and A. Wendel. 1992. A T cell–dependent experimental liver injury in mice inducible by concanavalin A. *J. Clin. Invest.* 90:196–203.
29. Osagawara, J., M. Watanabe-Fukunaga, A. Adachi, T. Matsuzawa, N. Kitamura, N. Itoh, T. Suda, and S. Nagata. 1993. Lethal effects of the anti-Fas antibody in mice. *Nature.* 364:806–809.
30. Watanabe, Y., M. Morita, and T. Akaike. 1996. Concanavalin A-induced perforin-mediated but not Fas-mediated hepatic injury. *Hepatology*. 24:702–710.
31. Wack, A., P. Corbella, N. Harker, I.N. Crispe, and D. Kioussis. 1997. Multiple sites of post-activation $CD8^+$ T cell disposal. *Eur. J. Immunol.* 27:577–583.
32. Abe, J., B.L. Kotzin, M.E. Melish, M.E. Glode, T. Kohsaka, and D.Y. Leung. 1992. Selective expansion of T cells expressing T cell receptor variable regions Vβ2 and Vβ8 in Kawasaki disease. *Proc. Natl. Acad. Sci. USA*. 89:4066–4069.
33. Furukawa, O.G., F. Fujiwara, and Y. Hamashima. 1985. Hepatomegaly and splenomegaly in Kawasaki disease. *Pediatr. Pathol.* 4:257–264.
34. Adachi, M., S. Suematsu, T. Kondo, J. Ogasawara, T. Tanaka, N. Yoshida, and S. Nagata. 1995. Targeted mutation in the Fas gene causes hyperplasia in peripheral lymphoid organs and liver. *Nat. Genet.* 11:294–300.